Scientific Research Publishing

Open Journal of Modern Hydrology, 2025, 15(2), 176-203
https://www.scirp.org/journal/ojmh
ISSN Online: 2163-0496
ISSN Print: 2163-0461

Hydrogeological Configuration of Grande Comore Island: Use of 3D Geological Modelling and Piezometry

Ibrahim Lhad Sosote[1,2*], Moctar Diaw[1], Ibrahima Mall[1,3], Konstantinos Chalikakis[4], Adriano Mayer[4], Remi Valois[4], Fatou Diop Ngom[1], Abdillahi Mze Ali[2]

[1]Departmet of Geology, Faculty of Sciences and Technique, Cheikh Anta DIOP University, Dakar, Senegal
[2]National Water Supply Society (SONEDE), Moroni, Comoros
[3]Applied Geosciences and Environment Department, Amadou Mahtar Mbow University, Dakar, Senegal
[4]Hydrogeology Laboratory, UMR 1114 EMMAH (AU-INRAE), Avignon University, Avignon, France
Email: *ibrahimlhad.sosote@ucad.edu.sn

How to cite this paper: Sosote, I.L., Diaw, M., Mall, I., Chalikakis, K., Mayer, A., Valois, R., Ngom, F.D. and Ali, A.M. (2025) Hydrogeological Configuration of Grande Comore Island: Use of 3D Geological Modelling and Piezometry. *Open Journal of Modern Hydrology*, **15**, 176-203.
https://doi.org/10.4236/ojmh.2025.152012

Received: December 15, 2024
Accepted: April 15, 2025
Published: April 18, 2025

Abstract

Hydrogeological modeling is an interesting and widely-used approach to improving our understanding of groundwater, both to test existing hypotheses on the behavior of hydrosystems and to predict their responses to various natural or man-made problems. Today, software such as Leapfrog Geo offers the possibility of building a 3D geological model with a more accurate representation of the subsurface. Statistical tools such as ordinary kriging can be used to simulate the spatial distribution of groundwater. These modeling approaches were combined to improve knowledge of the groundwater flow context within three massifs on the island of Grande Comore. The delineation of the 3D geometry of litho-stratigraphic units has enabled a more detailed conceptualization of groundwater flows in a complex volcanic environment. Piezometric interpolations were used to validate aquifer geometry. It has been demonstrated that an implicit geological model coupled with piezometry can provide very interesting information on the hydrogeological configuration of a volcanic massif. In the Karthala and Badjini massifs, the respective confined and semi-confined configurations of the aquifers are observed, with thicknesses that progressively decrease with distance from the coast. In the Grille massif, on the other hand, the aquifer configuration is unconfined, with thickness increasing with distance from the coast. In all three massifs, the flow of water in the underground hydrosystems is from the central part towards the coast, naturally following the geological configuration of the ground. It should be noted that the absence of data in the central parts of the massifs still leaves uncertainties about the geometry in these parts of the aquifers. However, the models

that have been established provide valid hypotheses for characterizing the hydrogeological configuration at the scale of each massif.

Keywords

Aquifer Configuration, Piezometry, 3D Geological Modelling, Flow, Grille Massif, Karthala Massif, Badjini Massif, Grande Comore Island

1. Introduction

The island of Grande Comore is made up of three different volcanic massifs. The Grille massif to the north, the Karthala massif in the centre, which is still active, and the older Badjini massif to the south. The island is deprived of surface water due to the geological nature and structure of the field. Rainwater rapidly infiltrates directly through the fissured or fractured volcanic formations on the surface, reaching the water table at depth.

The island's groundwater potential is considerable, but few investigations have been carried out to understand the hydrogeological configurations of the island's volcanic massifs. These include projects COI/79/005 and COI/86/001, supported by the United Nations Development Programme (UNDP) in the 1980s, which carried out some forty (40) wells and exploratory boreholes in coastal areas [1]; the pilot project for the management of public water services in rural areas on the island of Grande Comore (MPWS), financed by the French Development Agency (FDA) between 2012-2019, which has drilled eight deep wells that are a little way from the coast. Following the success of the MPWS project, the Water and Resilience to Climate Change (WRCC) project, initiated by the government and financed by the Green Climate Fund, plans to drill 6 new boreholes by 2030 to strengthen the groundwater monitoring and exploitation network. This work, which was not aimed at understanding hydrosystems, but rather at harnessing and exploiting them, revealed the potential of aquifers in certain areas of the island's massifs, and the threat of marine intrusion, which merited further study. Compiling all the intrinsic data to establish the hydrogeological configuration of the massifs was therefore an interesting way of understanding how the island's groundwater functions.

In addition, numerous geological and hydrogeological studies have been carried out to describe island volcanic aquifers. Volcanoes such as Teide in Spain [2]; [3], Karthala in the Comoros [4], Mauritius [5], Pico Island in the Azores archipelago [6], the Hawaiian archipelago [7], Piton de la Fournaise [8] and Mayotte [9] illustrate various types of aquifer.

The aim of this study is to conceptualize the hydrogeological systems of the island of Grande Comore, characterizing the nature of the aquifer formations, their geometry and the configuration of underground flows at the scale of each massif. Model conceptualization, which provides a qualitative framework for numerical model design, is a descriptive representation of a groundwater system

based on what is known about the area [10]. This study makes use of modelling, based essentially on the combination of intrinsic terrain parameters (borehole log, geological map) and groundwater level observations (piezometry). However, the absence of data in the central parts of the massifs makes it impossible to model the entire massifs. To minimize uncertainties, the study focused on areas with a good spatial distribution of data.

Implicit modeling techniques such as indicator kriging [11], radial basis function [12] and support vector classification [13]; [14] automates the construction of geological boundaries, thus reducing manual digitizing time. Among these, the radial basis function (RBF) algorithm is particularly popular with geological modellers and is available in several commercial software packages [15]. Aquifer conceptualization has traditionally relied on two-dimensional geological maps and cross-sections to develop an understanding of groundwater flow in three dimensions (3D). This process generally involves a significant simplification of the geological structure and can reduce understanding of the hydrogeological system [16]. The recent development of three-dimensional (3D) geological models from boreholes offers opportunities to improve the conceptualization of groundwater systems, with such models proving particularly useful for interpreting the complex geology often encountered in Quaternary aquifer systems [17]. The conceptualization of a three-dimensional geological model based on borehole lithological data began to convince hydrogeologists when Martin and Frind [18] successfully delineated a complex glacial aquifer system in Waterloo, Canada. Since then, the use of 3D geological models has become an established technique for representing subsurface geology, facilitating the understanding of complex geological settings [19]. The use of 3D geological models in the conceptualization of hydrogeological systems has become increasingly common (**Table 2**). They have been widely used in the modeling of hydrothermal springs, notably in New Zealand in volcanic contexts, virtually similar to that of the island of Grande Comore: Wairakei-Tauhara [20] [21]; Ohaaki [22]; Kawerau [23].

Today, with the growing demand for water by populations and the effects of climate change, water resources are increasingly threatened in terms of availability and quality [24]. This is why there is an urgent need to study and understand the functioning of underground hydrosystems on the island of Grande Comore, with the aim of proposing adaptive management to the effects of climate change and ensuring an adequate water supply for the population.

2. Study Area

2.1. Geographical Location and Climate

The island of Grande Comore is part of the Comoros archipelago, located at the northern entrance to the Mozambique Channel between Africa and Madagascar (**Figure 1**). It has a surface area of 1148 km^2, and measures 64 km at its longest and 24 km at its widest. The population is estimated at 379,367, spread across the island's twenty-eight communes [25].

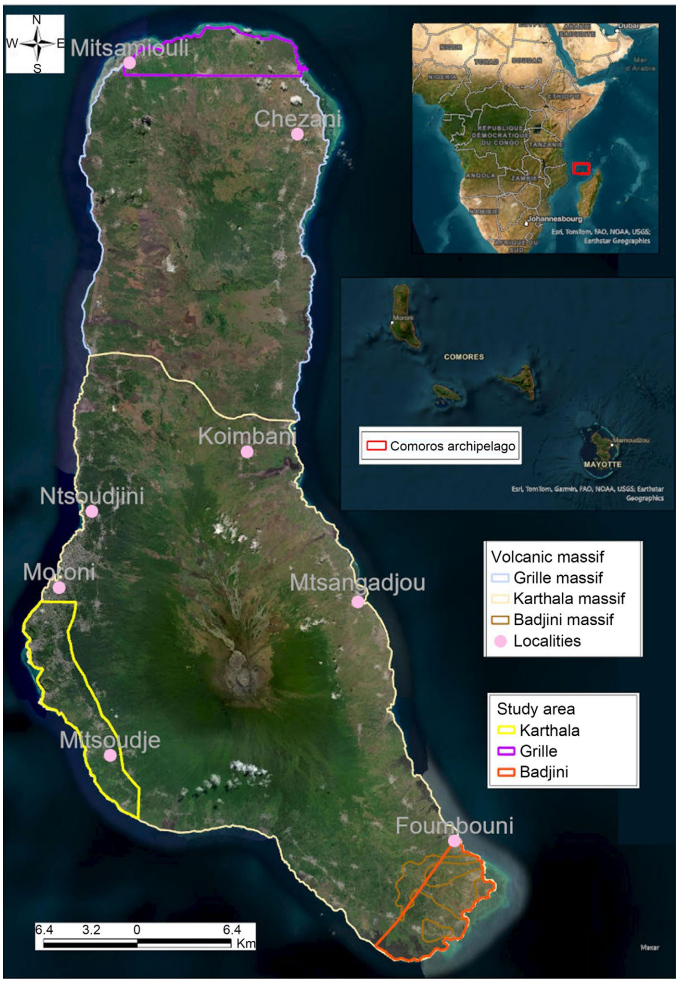

Figure 1. Geographical location, volcanic massifs on the island and areas. (Maxar satellite image)

The island's tropical oceanic climate is governed by the southeast trade winds and the northwest monsoon, which give rise to two contrasting seasons. A hot, humid season, corresponding to the austral summer, which lasts from November to April, and a cool, dry season, corresponding to the austral winter, which lasts from May to October.

The hot, humid season coincides with the rainy, cyclonic period. It is characterized by irregular north-to-north-westerly winds, relatively higher average annual temperatures (between 27˚C/28˚C with maximums of 33˚C recorded along the coast) and abundant rainfall, with recorded annual maximums of over 4m/year (**Figure 2**). On the other hand, during the dry season, the upwelling of cold polar air from the south to southeast through the Mozambique Channel usually results in lower temperatures (averaging 24˚C /25˚C) and more or less heavy rainfall on the highlands between August and September. The spatial distribution of rainfall is characterized by a high degree of spatial heterogeneity linked to geographical position: the windward slope, on the western flank, receives more rainfall than the leeward slope, on the eastern and south-eastern flanks (**Figure 2**).

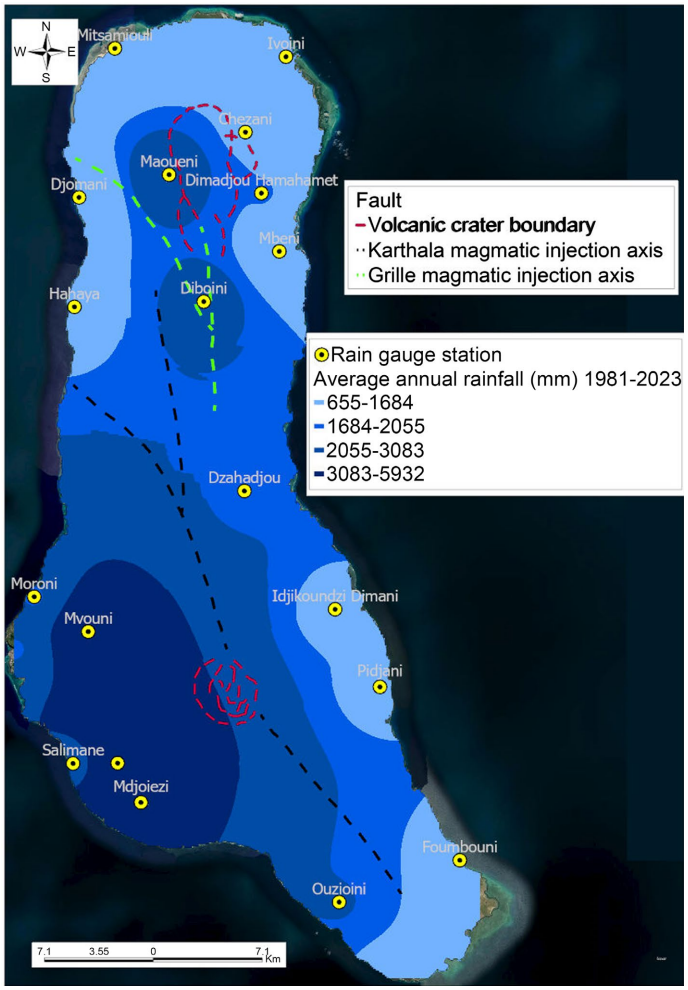

Figure 2. Fault and spatial distribution of rainfall. (Rainfall originate from Comoros National Agency for Civil Aviation and Meteorology)

2.2. Geology

The island of Grande Comore is made up exclusively of volcanic formations and deposits. The origin of volcanism on the islands of the Comoros archipelago has been the subject of numerous scientific studies, most of them based on several hypotheses. Successive works by Flower [26], Hajash and Armstrong [27], and Emerick and Duncan [28], based on geochronological studies carried out on the volcanism of northern Madagascar and the Comoros Islands, have shown that these volcanisms represent the trace of the operation of an active hot spot over the last ten million years. However, the work of Nougier [29], which highlighted the dispersion and overlap of ages measured on the various islands, refutes this thesis of volcanism linked to the operation of a hot spot. Since they question the migration of volcanic activity along the rift in favor of magmatic reactivation at different periods of ancient lithospheric fractures, traces of which can be found in the WNW-ESE faults to the north of Madagascar. Thus, the work of Upton [30], proposed an alternative hypothesis which states that the origin of the Comorian rift could be linked to the operation of a slow accretionary axis, therefore partially

emerged, cut by a series of transform faults.

In addition, radiochronological studies of volcanic formations carried out by Bachelery [31], based on morphological, conservation, alteration and petrological criteria for rocks on Grande Comore Island, have shown the existence of three types of volcanic massifs:

- **The small Badjini massif** outcrops in a few places in the southeastern part of the island (**Figure 3**). It is characterized by a northwest/southeast orientation and variable altitudes that can reach almost 700 m in the north. The Badjini massif is the oldest (Miocene), but is partly masked by recent Karthala emissions (**Figure 3**). It is clearly distinguishable by its geomorphology, the superficial alteration of its formations (**Photo 1(a)**) and, above all, the orientation of the magmatic intrusion:

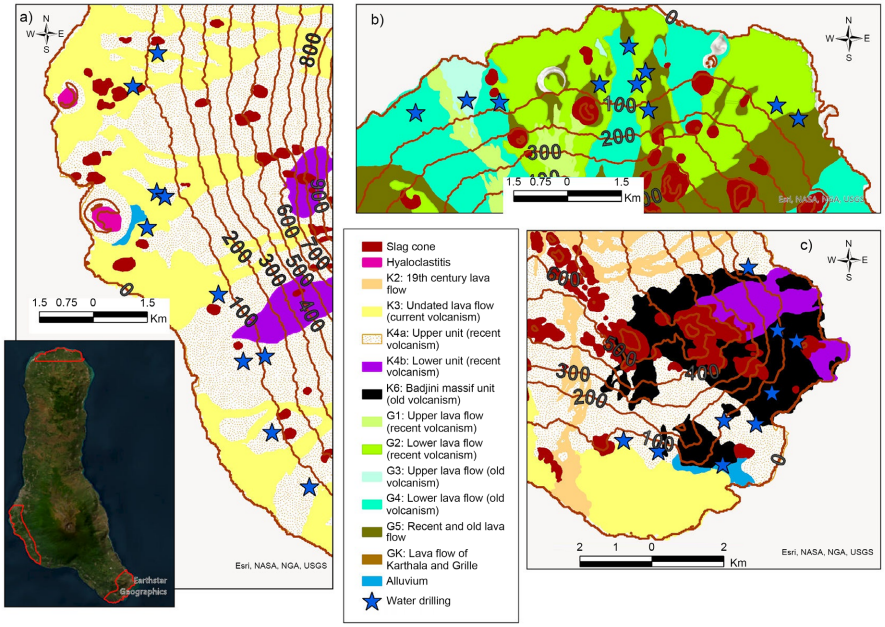

Figure 3. Geological map of the three study areas. [31]

Photo 1. Badjini massif, landscape of the study area.

- **The intermediate-age Grille massif** (Middle Pleistocene) has facies that are significantly older than those of Karthala. La Grille reaches an altitude of 1077 m and occupies the northern part of the island (**Figure 1**). Its summit zone is

occupied by numerous large scoriaceous cones built around the eruption points (Photo 2). The massif is characterized by volcanic deposits with a moderate to low degree of alteration. Projections from one of the volcano's most recent eruptions have been carbon-dated to 1300 ± 65 years BP (scoriaceous fallout covering the Sangani cone), while other wood charcoals associated with pottery fragments, also covered by a level of scoriaceous fallout (foot of the Sangani cone) have provided an age of 740 ± 130 years BP.

Photo 2. Grille massif, landscape of the study area.

- **The Karthala massif** covers the entire central and southern part of the island (Figure 1). It is a young active shield volcano (Quaternary), which last erupted in 2011. It is a very imposing massif, with maximum altitudes reaching 2361 m. It is characterized by the presence of highly irregular slopes (east and west) around Mount Karthala, which are extended by small coastal plains (Photo 3). The slopes are formed by two major rift zones (axes of magmatic injections) diametrically opposed on either side of the summit caldera (Figure 2). It is sometimes very difficult to distinguish the morphological dividing line from the Grille massif, and their shapes give the island its overall appearance

Photo 3. Karthala Massif, landscape of the study area.

2.3. Hydrogeology

The hydrogeological context of Grande Comore Island can be broken down into two hydrogeological domains: the coastal domain and that of the island's interior

[8] [32]-[38].

The coastal zone, characterized by the highly heterogeneous basic volcanic aquifer (fissured basalt and/or alluvium), is generally defined by low hydraulic gradients with piezometric levels close to mean sea level. This is the island's most heavily exploited hydrogeological zone, with almost all wells and boreholes drilled on the island tapping the base aquifer.

The interior domain is characterized by perched aquifers formed at the higher altitudes of the massifs by pyroclastics deposited in the relatively impermeable altered basalts. These underground hydrosystems are found in the Badjini and Grille massifs (**Photo 4**). They feed the few springs present in the island's high altitudes.

Photo 4. Spring in high altitudes, Badjini massif ((a) and (b)), Gille massif (c).

3. Methods and Materials

3.1. General Overview

The hydrogeological configurations of the island's massifs were developed through 3D geological modeling using Leapfrog Geo software and simulation of the spatial distribution of groundwater levels using ordinary kriging (**Figure 4**). In this study, three 3D geological models (one for each massif) were generated to characterize the lithological stratification of the terrain. Implicit geological modeling with radial basis functions is often insufficient to capture the extent of uncertainties due to its deterministic nature. However, the approach proposed in this study involves coupling geological modeling with piezometric level interpolation to properly represent underground hydrosystems and provide a representation of uncertainties. This method is particularly effective for modeling the geometry of aquifers characterized by irregular and complex structures. Stochastic techniques are designed to be compatible with implicit deterministic models of geological formations, bridging

the gap between deterministic and probabilistic modeling approaches [15]. By integrating piezometry into geological modelling frameworks, the approach improves the ability to predict and manage hydrogeological uncertainties.

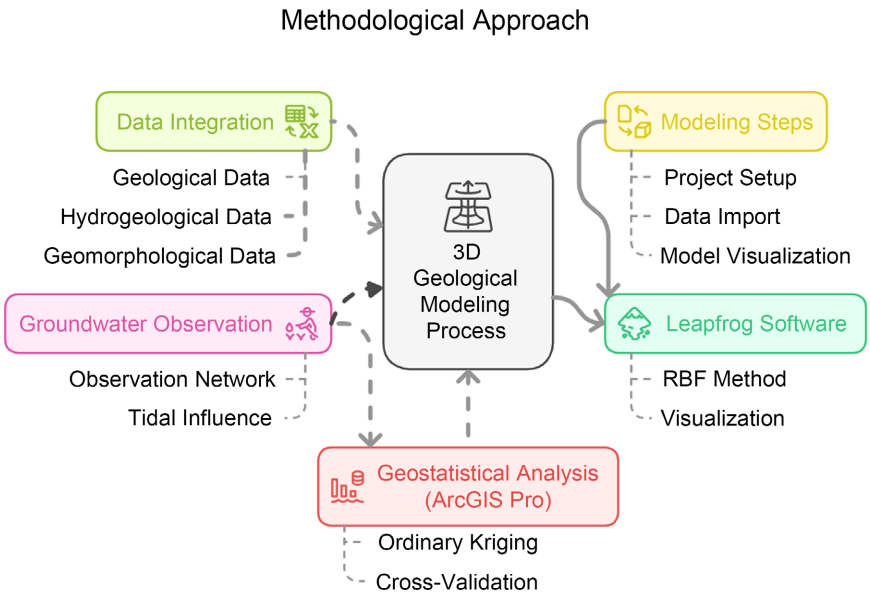

Figure 4. Methodological approach.

The island of Grande Comore is made up of three volcanic massifs. Due to the absence of boreholes in the central parts of the massifs, it is difficult to model an entire massif. Consequently, areas with a good spatial distribution of boreholes are selected (Table 1). One area in each massif is selected for this study. The main criterion used to choose the areas to be modeled is based on the proximity of several boreholes to each other.

Table 1. Modelled zones and lithological sets.

3D geological modeling						
Massifs	Surfaces (km²)	Drilling numbers	Minimum depth	Average depth	Maximum depth	Rock formations
Badjini	29.15	10	5	39.3	104	Clay gravel Hard basalt Alluvium Weathered basalt
Karthala	38.87	10	36	59.5	110.7	Gravel Weathered basalt Alluvium Hard basalt
La Grille	28.32	10	19.8	52.1	136.5	Weathered basalt Scoriaceous basalt Clay gravel Alluvium

3.2. Creating 3D Geological Models

In this study, we propose to build model blocks or training images using the Radial Basis Function (RBF), which is available today in several software packages. Leapfrog 2023 version 2.1 is used to create implicit geological models. Leapfrog is an excellent tool for modeling, visualizing and managing natural resources. It enables 3D conceptual models to be developed directly from borehole lithological data, GIS layers or other types of data. The idea is to combine all available geological data (geological and structural maps), hydrogeological data (lithological cross-sections of boreholes and wells) and geomorphological data (digital terrain models) to establish a 3D geological model of the subsurface at the scale of the study area. This approach, based on borehole data, offers several advantages [15]:

- Borehole data naturally represent the geological characteristics of the subsurface. Creating the geological model from borehole data ensures that the model accurately represents the geological features observed in the field;
- The model created from borehole data accurately represents the spatial distribution of lithological units;
- Borehole data often provide detailed information on specific areas of the subsurface. They allow us to see localized geological variations that may not be adequately represented in regional geological models;
- Models created from borehole data are generally more geologically accurate than synthetic or conceptual models. This can lead to more accurate geological simulations and predictions.

The 3D geological models created are used as interpretive geological models of the island's volcanic massifs, on which further piezometric analyses can be based. 3D geological models are widely used in the conceptualization of hydrogeological systems (**Table 2**) [39].

Table 2. Previous use of 3D geological models in the conceptualisation of hydrogeological systems.

Model application and type	Reference
An EarthVision 3D volume model was used to characterise hydrogeological units in a complex Quaternary esker aquifer.	[40]
The Victorian Department of Primary Industries, Australia, developed regional-scale 3D models to understand the distribution and history of mineral deposits, as well as energy and water resources.	[41]
3D geological visualisation tools were used to facilitate the development of robust and defensible conceptual groundwater models and were found to be cost effective.	[42]
Geological model data were used in a MODFLOW model of a geologically complex region of north-western Switzerland near Basel.	[43]
Key Canadian aquifers were modelled by the Geological Survey of Canada, resulting in increased understanding of groundwater resources, by integrating approaches including remote sensing, geophysics, 3D geological models, and 3D numerical hydrogeological models into basin analyses.	[44]
High-resolution airborne geophysical data were integrated into local 3D hydrogeological models.	[45]

Continued

Three-dimensional models were developed to represent the distributions of key sediments and static groundwater level in the lower Wairau Plain, New Zealand.	[46]
High-resolution 3D modelling was used to characterise the complex geological environment of the Bitterfeld/Wolfen megasite in the eastern part of Germany.	[16]
Three-dimensional hydrostratigraphy and groundwater flow models in complex Quaternary deposits and weathered/fractured bedrock: evaluating increasing model complexity (Sodankylä in northern Finland).	[47]

3.3. Groundwater Observation Network

Groundwater is observed through a network of wells and boreholes. Most observation structures are equipped with multi-parameter sensors connected to Seba Hydrométrie data loggers (Photo 5). The system continuously measures and records the level of the water table. In all three massifs, the water table is influenced to a greater or lesser extent by tidal waves. As proposed by Clifford Voss and Souza [48], each piezometric observation point should be subjected to a period of observation in order to obtain a corrected static level from the tidal curve and recurrent oscillations in the water table, and then calculate the piezometric level. The piezometric values are shown in Table 3.

Photo 5. Device for measuring, recording and collecting piezometric data.

Table 3. Piezometric levels observed in the study areas.

Grille Massif		
Locations	Names	Observed piezometric levels (m) in January 2024
Mitsamihouli	ONU2	6.21
Hadawa	ONU27	10.5
Ouella-Mitsamihouli	ONU8	5.25

Continued

Ouella-Mitsamihouli	F4 wel	19.77
Bangoi Kouni	ONU43	6.67
Ivoini	ONU26	9.92
Ivoini	ONU7	7.48
	Karthala Massif	
Mitsoudjé	F8 Mit	11
Mkazi	F13	13
Ndrouani	PZ Nr	5
Mdé	TP1	11
Vouvouni	ONU4	9
Vouvouni	TP5	10
Chouani	ONU9	13
Séléa	ONU35	17
Mitsoudjé	ONU37	8
Mdjoiyezi	F12	12
Bangoi-Hambou	ONU38	11
	Badjini Massif	
Midjédjén	F11	17
Malé	PZ M	9
Malé	ONU18	8
Ouropveni	ONU44	6
Ouropveni	ONU17	11
Simaboini	ONU10	9
Dzahadjou	ONU42	8
Foumbouni	ONU3	10
Chindini	ONU15	7

3.4. Geostatistical Analysis of Piezometry

Once the geological model has been constructed, various geostatistical algorithms can be used to simulate water levels in aquifer formations. Among these algorithms, kriging stands out as a geostatistical interpolation technique that uses the statistical properties of measured points. It quantifies the spatial autocorrelation between measured points and takes into account the spatial configuration of sampling points around the prediction location [49] [50]. In recent

decades, kriging has become a fundamental tool in geostatistics [51]. The aim of kriging is to estimate the value of a random variable at one or more unsampled points from more or less sparse samples [52]. It exploits the spatial correlation between spatially neighboring observations to predict unsampled locations [53]. To create a surface or map of a phenomenon, predictions are made for locations within the study area on the basis of the semi-variogram and the spatial arrangement of values measured nearby [54] [55].

Kriging covers a range of spatial least-squares prediction methods. However, ordinary kriging (KO) is used in this study to produce piezometric maps. The choice of this method is based on the reliability of the results. Ordinary kriging is the most robust and widely used method [52]. It estimates the value of the variable at a given point from values at surrounding stations and from a variogram model for the variable [55]-[57]. The variogram defines the relationship between variability (or geological distance) and offset distance (or Euclidean distance) [58]. It illustrates the spatial continuity or correlation of the phenomena studied [59].

ArcGIS Pro software version 3.3.1 is used for piezometric interpolations. ArcGIS Pro's geostatistical assistance tool is used to generate interpolation models adapted to the type of data and to assess model quality using the cross-validation method [60]. After testing several semi-variogram models, the hole effect model is chosen, as it is consistent and cross-validation yields lower errors. Hole effect structures most often indicate a form of cyclicity or periodicity, which is a common and legitimate spatial feature in geology [58]. Cross-validation is used to assess the quality of model predictions at new locations. The model with the lowest error is the best-fitting interpolation model [61] [62].

4. Results

4.1 Overall Aquifer Configuration

The FRB algorithm was used to build explanatory 3D models of the terrain based on lithological data from the boreholes. The geological models thus created made it possible to visualize the extent and thickness of geological formations, and to identify potential aquifer formations. Piezometric interpolation was used to simulate the spatial distribution of the water table in the study areas, with the delivery of uncertainties. The combination of these two approaches enabled us to characterize the configuration and nature of the island's aquifers, which differ from one massif to another.

4.2. Hydrogeological Configuration of the Grille Massif

The northernmost part of the Grille massif was chosen on the basis of a much denser network of wells and boreholes. The implicit geological model of La Grille indicates that the first horizons of the massif are characterized by fairly scattered clayey gravels. These gravels, essentially made up of more or less altered pyroclastites of varying grain sizes (ash, lapillis, slag and volcanic tuffs), were probably laid down by recent volcanism at La Grille. Beneath these clayey gravels lies a series of

more or less altered vacuolar basalts, outcropping in a few places on the massif (Figure 5). They probably originate from ancient volcanism. A little deeper down, we find a thin layer of alluvium deposited in the scoriaceous basalts. All along the north coast of the massif, particularly in the Mitsamihouli locality, alluvial deposits consisting mainly of white sand from the beautiful beaches of the north coast.

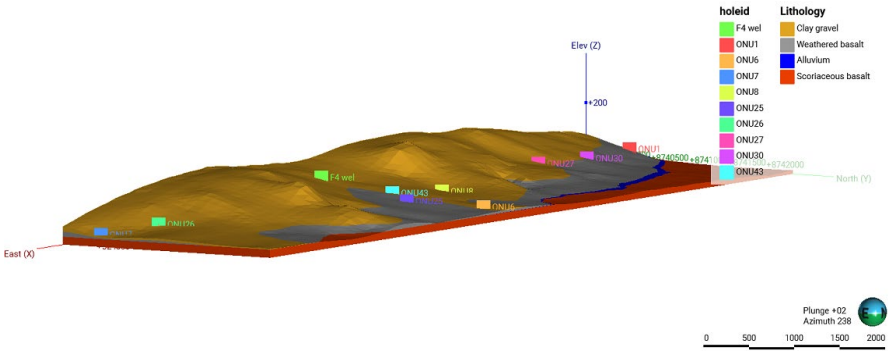

Figure 5. Grille 3D geological model.

As in all three massifs, the geology of the Grille shows a gradual decrease in the thickness of gravel and basalt towards the coast. This geometric configuration of the dome-shaped formations clearly indicates that they were laid down by a series of volcanic eruptions from the central zone of the massif towards the coast. The alluvium deposited in the scoriaceous basalt, successively covered by various volcanic envelopes, was probably deposited by the sea, as it is close to mean sea level with a relatively flat surface.

The 3D geological model of the Grille massif is based on the assumption that the massif is divided into two hydrogeological domains: the perched aquifer at high altitudes and the deep basal aquifer.

Perched aquifers are particularly noticeable in the central zone of the massif, which is not included in the geological model due to a lack of data. However, we can draw on the modelled area to try and explain the reason for their existence. These pockets of water permanently feed the few springs in the massif, the most famous of which are those of Maoueni (660 m altitude) and Helendjé (669 m altitude). However, their flow remains low and varies according to the season. They are made up of a succession of clayey gravels resulting from the alteration of pyroclastites and basalts. These basalts, often referred to as dykes, are at the origin of these perched aquifers, as they generally act as a hydraulic barrier, reducing the vertical circulation of water and thus compartmentalizing the aquifers [63].

On the other hand, the base aquifer is generally tapped by wells in the coastal zone and boreholes in the parts slightly far from the coast (Figure 6). However, the absence of deep boreholes in the central part means that indications of the continuity, extension and configuration of this base aquifer towards the central zone of the massif remain hypothetical. The Grille base aquifer is close to sea level in the coastal zone. It consists mainly of scoriaceous and vacuolar basalt, with some alluvium in places. Basalts generally have very low matrix permeabil-

ity, and their aquifer properties are closely linked to their emplacement, fissuring and fracturing conditions [9]. However, their degree of alteration also plays an important role in the emplacement of underground reserves. The basal aquifer is predominantly scoriaceous basalt in the coastal area, but becomes multi-layered as one moves away from the coast, consisting mainly of altered and scoriaceous basalt.

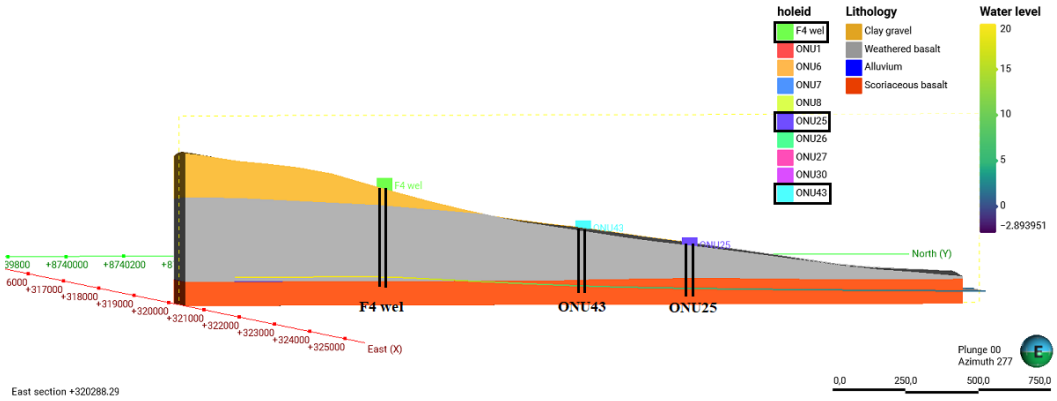

Figure 6. South-north hydro-stratigraphic section around F4 wel, ONU43 and ONU25.

The semi-variogram generated from the Hole Effect interpolation model, which takes into account the aquifer's heterogeneity, shows that the piezometric observation data are generally well matched to the model (**Figure 7(c)**). We can therefore assume that the Grille base water table is continuous over the entire study area.

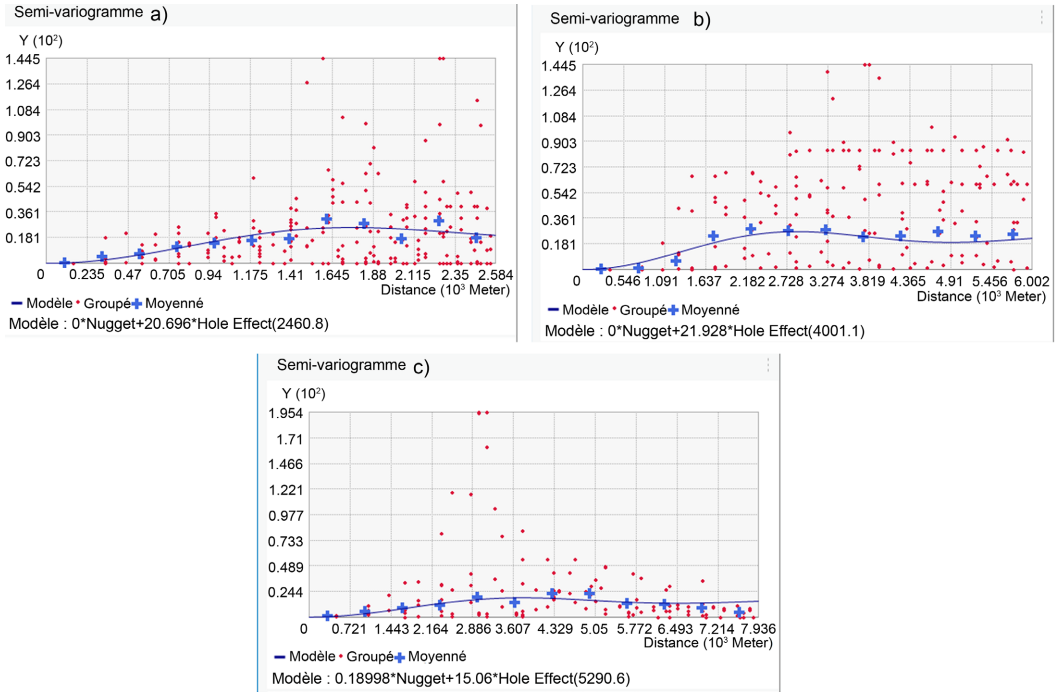

Figure 7. Semi-variogram of piezometric interpolations, (a) Badjini, (b) Karthala and (c) Grille.

The piezometry of this northern part of the Grille massif indicates that the general flow of the water table is from the central part of the massif towards the coast, with a calculated hydraulic gradient of around 10^{-3} (**Figure 8(a)**). However, uncertainties are observed in the remote parts of the observation points, which are affected by somewhat high standard forecast errors (**Figure 8(b)**), which is quite normal. As with topography, piezometry generally increases with distance from the coast.

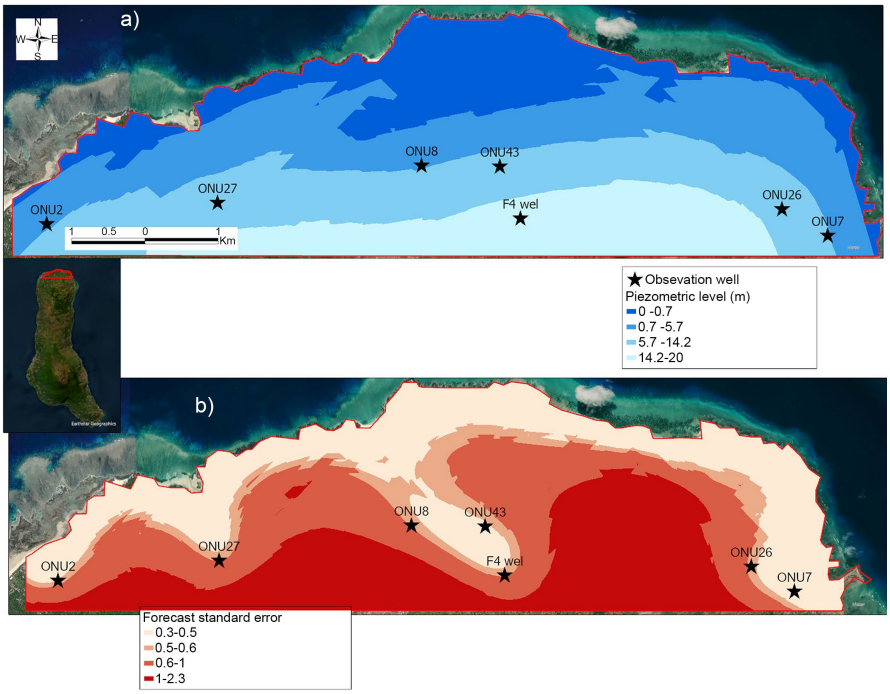

Figure 8. (a) Piezometric map; (b) Standard forecast errors.

Rainwater seeping through the cracked and fractured gravels and basalts can reach the base aquifer at depth. In addition to the geological nature of the aquifer, it has been found that in the coastal zone, the base aquifer lies at altitudes close to mean sea level, with a very low hydraulic gradient, which exposes the Grille base aquifer to the phenomenon of marine intrusion. Thus, piezometry varies in accordance with the tidal wave; during high tide, the water level rises, and during low tide, it falls. This event has repercussions on groundwater flow, increasing salinity and altering water quality.

In addition, setting the piezometric level in the implicit geological model gave us an idea of the thickness of the water table within the aquifer formations, and therefore the geometry of the aquifer. The north-south section between borehole F4 wel and well ONU25 clearly illustrates the geometry of the aquifer (**Figure 6**). This is a heterogeneous basaltic aquifer, in which the entire thickness of the formations that make it up are not saturated with water, despite abundant and regular rainfall. This can probably be explained by the lateral (south-north) flow of the aquifer, favoured by fissure permeability. Consequently, in the coastal zone, close

to the water table's outlet (the sea), the upper part of the scoriaceous basalt is not saturated with water, as the water table discharges continuously into the sea. Like the piezometry, the saturated thickness increases as we approach the central zone, which is favorable to groundwater recharge. So the flow pattern of the water table within the aquifer does not depend on the geometry of the aquifer formations, but rather on their high permeabilities. This hydrogeological configuration indicates that the heterogeneous, multi-layered Grille base aquifer is unconfined. Recharge occurs preferentially in the central part of the massif (which receives the most rainfall), and water flows laterally through the aquifer's connected pores and fissures towards the coast and out to sea. This type of aquifer has a very low water residence time. In the coastal area, the aquifer is characterized by a lens-shaped water table floating on seawater, with a very gently dipping piezometric surface (**Figure 6**). This hydrogeological configuration of the Grille massif is similar to that of the Hawaiian model, insofar as a distinction is made between the base water table and perched water tables, which are encountered at altitudes higher than the roof of the base water table [7] [64].

The wells that tap 3 m maximum the scoriaceous basalt aquifer (ONU7, ONU26, ONU27, ONU8, ONU2 and ONU43) in the coastal area are operated at low flow rates (10 to 20 m^3/h) because the water is brackish. Borehole F4 wel, on the other hand, is a little further from the coast, and taps 18 m of freshwater in the altered and scoriaceous basalt aquifer (**Figure 6**) with a flow rate of 108 m^3/h. This spatial distribution of flow rates shows that the aquifer is both qualitatively and quantitatively productive further from the coast. This confirms the identified pattern of groundwater flow, which runs from the central part of the massif towards the coast.

4.3. Hydrogeological Configuration of the Karthala Massif

The hydrogeological study of the Karthala massif was carried out on the western slope of the massif, more specifically in the Bambao-Hambou plain between the capital Moroni and the village of Bangoi Hambou. This part of the massif is densely populated, and groundwater is therefore much in demand for the population's water supply. The Comorian Water Exploitation and Distribution Company (SONEDE) operates 4 wells and 2 boreholes in the area. In 2023, these facilities produced a water volume of 5871549 m^3 [65]. 3D modelling of the subsurface has identified four stratigraphic units represented from top to bottom by gravels, weathered basalts, alluvium and hard basalts (**Figure 9**).

On the surface, the gravels overlying the basalts are very heterogeneous. The basalts, with their slightly blunted surface character, appear as a variably altered unit. They consist mainly of flows and pyroclastites resulting from magmatic explosions (lapillis and scoriaceous bombs), phreatic or phreato-magmatic explosions (ash deposits with lapillis and boulders). These altered basalts, which represent the upper unit of recent volcanism observed in the Karthala massif, cover the very heterogeneous alluvial formation at depth, which rests concordantly on the hard basalts. The latter are probably derived from the lower unit of recent volcanism.

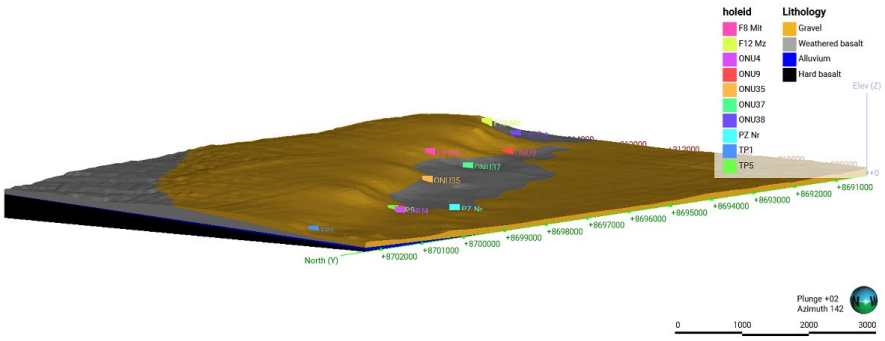

Figure 9. 3D geology of the Bambao plain (Karthala massif).

At the scale of the Karthala massif, there are no springs at high altitudes. The main aquifer formation is represented by alluvium, which has been tapped at depth by virtually all the wells and boreholes in the study area. This highly heterogeneous alluvium is composed of slag, pebbles and fine to coarse gravel sands. Like the topography, the alluvial layer has a seaward sloping geometry. The alluvial aquifer is framed at the base by hard basalts and above by weathered basalts. Its thickness gradually decreases in favour of the basalts as one moves away from the coast towards the central zone of the massif (west-east) and from north to south (**Figure 9**). These epontes may also have interesting hydraulic properties, which can increase the aquifer potential or the storage of groundwater.

The piezometric observations fit the hole-effect interpolation model perfectly (**Figure 7(b)**). The piezometric map generated is well representative, with low standard forecast errors (**Figure 10**). It also shows that the water table flows from the central part of the massif towards the coast, with a calculated hydraulic gradient of around 10^{-3}.

Geological modelling gives an idea of what the geometry of the aquifer might be. However, it is the piezometry fixed in the implicit geological model that definitively determines the geometry of the alluvial aquifer. In fact, the piezometry and the roof of the alluvial formation are practically at the same altitude, so we can say that the alluvial aquifer is saturated throughout its entire thickness. The west-east section between wells TP5 and ONU4 clearly illustrates the geometry of this aquifer (**Figure 11**). However, beyond one kilometer from TP5 towards the interior of the island in general, the piezometry is not at the same altitude as the aquifer roof due to the absence of observation boreholes, and this is expressed by higher standard errors in piezometric predictions. However, the lateral continuity of the aquifer towards the central part of the Karthala massif has been proven with the same geometry as that obtained in this study using geophysical techniques [4]. The thickness of the aquifer decreases progressively away from the coast, unlike the basalts it surrounds, and this inclines the alluvial aquifer towards the sea (**Figure 11**). As the piezometry and roof of the alluvial aquifer are found at the same altitudes despite the dip of the terrain, we could validate the hypothesis of a confined base aquifer with possible lateral continuity towards the central part and a general flow of the water table from the central part of the massif towards the

coast. The central part of the massif is characterized by very high rainfall and the presence of geological structures such as craters, rift zones and caves, favoring direct recharge. Rainwater infiltrates and flows through the aquifer towards the coast, naturally following the topography of the land. The production capacity (more than 5 871 549 m^3 in 2023) of the wells and boreholes that tap this aquifer reinforces the idea of a very powerful confined aquifer. For example, the TP5 and ONU4 wells (Figure 11) have aquifer thicknesses of 14 m and 8 m respectively, with operating rates of 400 m^3/h for TP5 and 120 m^3/h for ONU4.

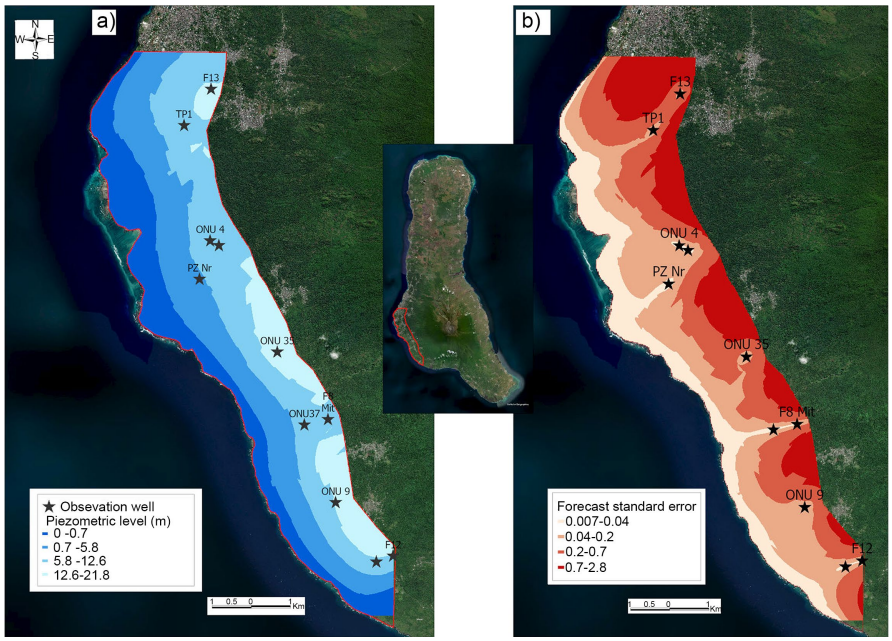

Figure 10. (a) Piezometric map of the Karthala massif, (b) Standard forecast errors. (Source: the author)

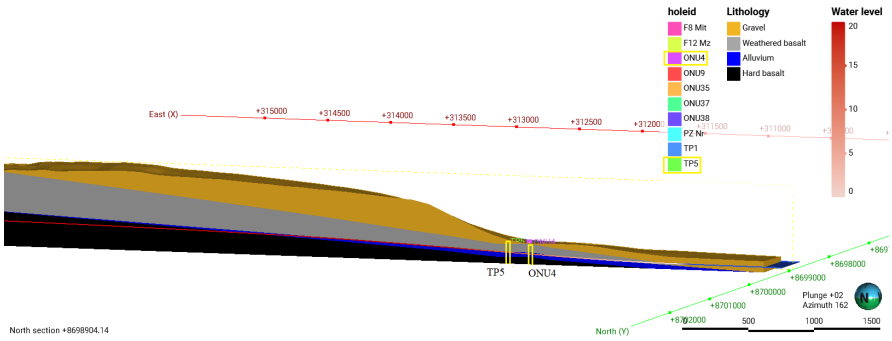

Figure 11. Eastwest hydro-stratigraphic section around TP5 and ONU4.

4.4. Hydrogeological Configuration of the Badjini Massif

Geological modelling has also enabled us to distinguish, from top to bottom, four stratigraphic units in the Badjini massif: clayey gravels, hard basalts, alluvium and altered basalts. Clayey gravels are made up of pyroclastites and highly altered volcanic flows. The more or less weathered basalts found in the northern part of the

massif are the result of projections and flows from the recent Karthala volcanism. These basalts overlie the ancient Badjini volcanic formations. At depth, the basalts generally cover the alluvium, which is essentially composed of pebbles, slag and sand resting on weathered basalts. Hard basalts outcrop on the surface in a few areas of the massif (Figure 12).

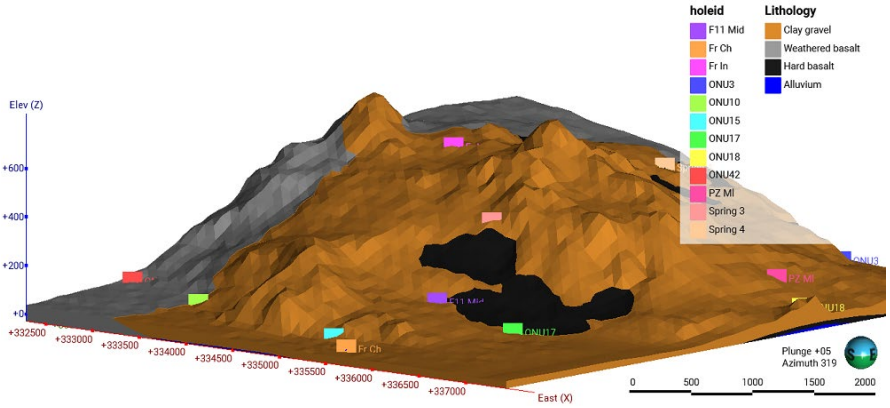

Figure 12. 3D geology of Badjini massif.

As in the Grille massif, two hydrogeological domains can also be distinguished in the small Badjini massif: the perched aquifers at high altitudes and the deep basal aquifer.

Perched hydrosystems are pockets of water created by the alterites that line the contact surface between the gravels and the relatively impermeable hard basalts (Figure 12). On certain levels, this prevents water from circulating vertically towards the base water table and favours the emergence of springs in the higher altitudes of the massif, as in the case of Gnambeni (Spring 3) and Kopvé (Spring 4) (Figure 12). These springs have relatively low flow rates, which vary according to the season.

At depth, there are two aquifer formations, the weathered basalt in a small part to the southwest and the alluvium that occupies a large part of the study area. The two aquifers are probably hydraulically linked. The basalt is tapped by two wells (ONU42 and ONU10) with low production rates due to the salinity of the water. The massif's main aquifer is the alluvial aquifer, mainly composed of highly heterogeneous alluvium. The thickness of the alluvium decreases in favor of the basalts as one moves away from the coastal zone towards the center of the massif. Like the topography, the alluvial layer slopes towards the sea, forming a sloping geometry. Most of the wells and boreholes drilled in the area tap this alluvial aquifer. For example, at borehole F11 Mid, we have an alluvial aquifer thickness of 23 m and an operating flow rate set at 108 m^3/h.

The piezometric map generated by the hole-effect interpolation model shows that the piezometric data fit the model perfectly (Figure 7(a)), so we can assume lateral continuity of the water table in this part of the study. Like the other massifs, the piezometry also indicates a general flow of the water table from the central

part of the massif towards the coast, with a calculated hydraulic gradient of around 10^{-3}. However, piezometric uncertainties exist in places where standard forecast errors are high (Figure 14).

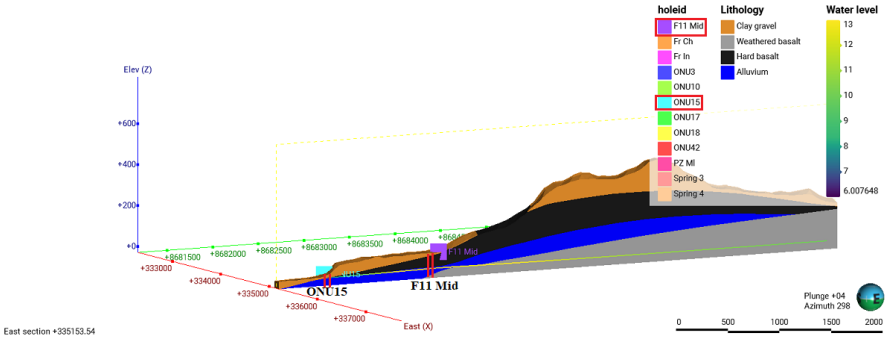

Figure 13. South-north hydro-stratigraphic section around ONU15 and F11 Mid.

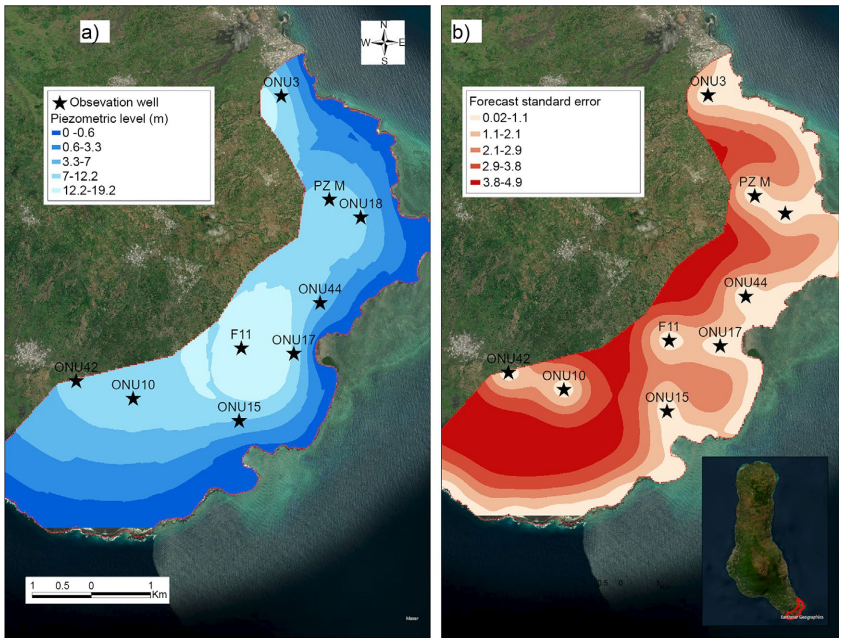

Figure 14. (a) Piezometric map of the Badjini base water table, (b) Map of standard errors. (Source: the author)

As with the western flank of Karthala, the aquifer roof elevations increase with distance from the coast. Figure 13 clearly illustrates the geometry of the Badjini basal aquifer. In general, the aquifer roof elevations are close to those of the piezometry, but this is not the case beyond borehole F11 towards the interior of the island, as the standard errors of piezometric prediction are higher due to the absence of observation boreholes. It can be assumed that the entire thickness of the alluvial aquifer in the study area is almost saturated with water. The seaward slope of the piezometer can be explained by the gradual reduction in thickness of the alluvial aquifer as the altitude rises, in favour of the basalts (Figure 13). Consequently, the flow is from the central part to the coast. This hydrogeological configuration

suggests that the springs observed at higher altitudes are probably hydraulically linked to the base aquifer. The Badjini underground hydrosystem resembles a semi-confined aquifer, with much of the recharge taking place in the central part of the massif, where structures such as dykes, craters, faults and high rainfall are present.

5. Discussion

This study proposes a way of using intrinsic geological and hydrogeological information to model the hydrogeological configuration of a volcanic massif. It begins by using borehole lithology and topography to build the implicit geological model, followed by the development of a predictive model to simulate the spatial distribution of water levels within the aquifer. This work offers insights into the implementation details of the proposed algorithms for studying aquifer configuration.

Implicit geological modeling offers several advantages, including the ability to generate models quickly by creating geological contact surfaces from limited data, integrating many types of data, and reducing the need for manual intervention through automation. Implicit geological modelling may encounter difficulties in effectively representing complex geological features, particularly when input data is limited (as in this study), which could lead to less accurate geological interpretations.

Although there are many advantages to generating the geological model from borehole data, this method is open to legitimate criticism. Drilling data generally covers a restricted area and may not fully represent geological heterogeneity at depth. The discrete nature of drilling data, providing point measurements rather than continuous spatial information, can pose challenges in capturing the continuity and spatial correlation of geological features in the model, particularly in regions with limited data coverage.

In short, using drilling data to create an implicit geological model has advantages in terms of geological realism and direct representation of field observations. However, it is important to take into account the limitations and reliability of the data source to maintain modeling accuracy. By combining drilling data with other geological information and implementing appropriate controls, it is possible to mitigate the difficulties encountered and improve the efficiency of the geological model.

Although it enables the stratification of geological formations to be visualized in 3D, the implicit geological model alone does not, in some cases, enable the hydrogeological system to be conceptualized, especially in a complex geological environment. For this reason, we have proposed in this study a combination of implicit geological modelling with piezometric interpolation to properly represent aquifers.

Ordinary kriging is used for piezometric interpolation. Despite its advantages, it has limitations that can affect its application. The major challenge is the need for a lot of well-dispersed data in the area to provide reliable estimates. When data

are sparsely sampled, estimates can become less precise, leading to higher kriging variance in areas where data coverage is limited, as is the case in this study.

The hypothesis of the continuity of the base aquifer in the central parts of the massifs is characterized by the presence in the central parts of geological structures such as craters and faults, and by regular, abundant rainfall. Consequently, the central parts of massifs are likely to be areas of preferential groundwater recharge. The geometries of the aquifers studied, the direction of flow and the flow rates applied in the wells and boreholes all support the hypothesis of a hydraulic connection between the central parts of the massifs for which no data are available and the areas studied (coastal zones).

6. Conclusions

The aim of this study was to model aquifer configuration using geostatistical interpolations. Modeling volcanic formations is challenging due to their complex geometries. Implicit geological modeling is a deterministic interpretation that defines the main lithological zones based on geological knowledge and borehole samples. However, there is always uncertainty as to the actual extent of the lithological zones. A probabilistic technique involving piezometric level simulation has been proposed to properly conceptualize aquifer geometries in order to understand how they function.

Through the combination of 3D implicit geological modelling and geostatistical analysis of piezometry, the results demonstrated the presence of a deep basal aquifer in the Karthala massif, which is probably continuous towards the central part with a geometry inclined towards the sea. Whereas, in the Grille and Badjini massifs, both perched hydrosystems (at high altitudes) and deep base hydrosystems were found to be present, which may be completely isolated (Grille massif) or sometimes hydraulically continuous (Badjini massif). In the Karthala Massif and the ancient Badjini Massif, the aquifers are respectively confined and semi-confined, with thickness configurations that diminish with distance from the coast. In contrast, the base aquifer of the Grille massif is unconfined, with a thickness configuration that increases with distance from the coast.

It was also found that in all three massifs, groundwater flows from the central part towards the coast. It is accepted that groundwater is probably recharged from the central areas of the massifs, which are often characterized by high rainfall and the presence of specific geological structures such as faults, caves, calderas and craters, which can encourage the direct infiltration of rainwater into underground hydrosystems. It should be recalled that this study was very interesting, as it enabled us to better characterize the geometry and configuration of the aquifers, and to gain a good understanding, from a hydraulic point of view, of how these aquifers could function, with the aim of better ensuring their rational and sustainable management in the face of the major challenges of increased exploitation of resources, degradation of water quality and climate change.

This study could contribute to rational water management, helping local authorities to identify areas with high groundwater potential, areas to be exploited with cau-

tion and the water flow context. By highlighting the different aquifer structures on Grande Comore Island, the study also opens up the possibility of addressing other groundwater-related themes, such as groundwater hydrodynamics, saline intrusion, water quality and recharge processes.

Acknowledgements

We acknowledge the following institutions for their support and their fruitful scientific cooperation in this research: Hydrogeology Laboratory of Avignon University, Department of Geology Cheikh Anta DIOP University, Seequent Society and National Water Supply Society of Comoros.

Conflicts of Interest

The authors declare no conflicts of interest regarding the publication of this paper.

References

[1] Marini, D. (1990) Résultas et interpretations d'une campagne de pompage d'essai sur des puits dans les aquifères de base de la Grande Comore. DCTD, Technique COI/79/005 et COI/86/001.

[2] Ecker, A. (1976) Groundwater Behaviour in Tenerife, Volcanic Island (Canary Islands, Spain). *Journal of Hydrology*, **28**, 73-86. https://doi.org/10.1016/0022-1694(76)90053-6

[3] Custodio Gimena, E. (2025) Geohidrología de terrenos e islas volcánicas. https://dialnet.unirioja.es/servlet/libro?codigo=195829

[4] Savin, C., Ritz, M., Join, J. and Bachelery, P. (2001) Hydrothermal System Mapped by CSAMT on Karthala Volcano, Grande Comore Island, Indian Ocean. *Journal of Applied Geophysics*, **48**, 143-152. https://doi.org/10.1016/s0926-9851(01)00078-7

[5] Bret, J., Join, L. and Coudray, J. (2000) Investigation on Deep Water Resources by Tunnels within the "Piton des Neiges" Volcano, Reunion Island. In: Sililo, O., Ed., *Groundwater*: *Past Achievements and Future Challenges*, A. A. Balkema, 1103-1106.

[6] Cruz, V. and Silva, O. (2001) Hydrogeologic Framework of Pico Island, Azores, Portugal. *Hydrogeology Journal*, **9**, 177-189. https://doi.org/10.1007/s100400000106

[7] Izuka, S.K. and Gingerich, S.B. (2003) A Thick Lens of Fresh Groundwater in the Southern Lihue Basin, Kauai, Hawaii, USA. *Hydrogeology Journal*, **11**, 240-248. https://doi.org/10.1007/s10040-002-0233-5

[8] Join, J., Folio, J., Bourhane, A. and Comte, J. (2015) Groundwater Resources on Active Basaltic Volcanoes: Conceptual Models from La Réunion Island and Grande Comore. In: Bachelery, P., Lenat, J.F., Di Muro, A. and Michon, L., Eds., *Active Volcanoes of the World*, Springer, 61-70. https://doi.org/10.1007/978-3-642-31395-0_5

[9] Lachassagne, P., Aunay, B., Frissant, N., Guilbert, M. and Malard, A. (2014) High-resolution Conceptual Hydrogeological Model of Complex Basaltic Volcanic Islands: A Mayotte, Comoros, Case Study. *Terra Nova*, **26**, 307-321. https://doi.org/10.1111/ter.12102

[10] Anderson, M.P., Woessner, W.W. and Hunt, R.J. (2015) Modeling Purpose and Conceptual Model. In: Anderson, M.P., Woessner, W.W. and Hunt, R.J., Eds., *Applied Groundwater Modeling*, Elsevier, 27-67. https://doi.org/10.1016/b978-0-08-091638-5.00002-x

[11] Ziegel, E.R., Deutsch, C.V. and Journel, A.G. (1998) Geostatistical Software Library and User's Guide. *Technometrics*, **40**, 357. https://doi.org/10.2307/1270548

[12] Franke, R. (1982) Smooth Interpolation of Scattered Data by Local Thin Plate Splines. *Computers & Mathematics with Applications*, **8**, 273-281. https://doi.org/10.1016/0898-1221(82)90009-8

[13] Smirnoff, A., Boisvert, E. and Paradis, S.J. (2008) Support Vector Machine for 3D Modelling from Sparse Geological Information of Various Origins. *Computers & Geosciences*, **34**, 127-143. https://doi.org/10.1016/j.cageo.2006.12.008

[14] Hardy, R.L. (1971) Multiquadric Equations of Topography and Other Irregular Surfaces. *Journal of Geophysical Research*, **76**, 1905-1915. https://doi.org/10.1029/jb076i008p01905

[15] Zhexenbayeva, A., Madani, N., Renard, P. and Straubhaar, J. (2024) Using Multiple-Point Geostatistics for Geomodeling of a Vein-Type Gold Deposit. *Applied Computing and Geosciences*, **23**, Article ID: 100177. https://doi.org/10.1016/j.acags.2024.100177

[16] Wycisk, P., Hubert, T., Gossel, W. and Neumann, C. (2009) High-resolution 3D Spatial Modelling of Complex Geological Structures for an Environmental Risk Assessment of Abundant Mining and Industrial Megasites. *Computers & Geosciences*, **35**, 165-182. https://doi.org/10.1016/j.cageo.2007.09.001

[17] Burke, H., Morgan, D., Kessler, H. and Cooper, A. (2025) A 3D Geological Model of the Superficial Deposits of the Holderness Area. https://www.semanticscholar.org/paper/A-3D-geological-model-of-the-superficial-deposits-Burke-Morgan/d7352283fc4e51abba596e7166e05536a941beac

[18] Martin, P.J. and Frind, E.G. (1998) Modeling a Complex Multi-Aquifer System: The Waterloo Moraine. *Groundwater*, **36**, 679-690. https://doi.org/10.1111/j.1745-6584.1998.tb02843.x

[19] Berg, R.C., Mathers, S.J., Kessler, H. and Keefer, D.A. (2011) Synopsis of Current Three-Dimensional Geological Mapping and Modeling in Geological Survey Organizations. Illinois State Geological Survey Circular, Vol. 578.

[20] Rosenberg, M.D., Bignall, G. and Rae, A.J. (2009) The Geological Framework of the Wairakei-Tauhara Geothermal System, New Zealand. *Geothermics*, **38**, 72-84. https://doi.org/10.1016/j.geothermics.2009.01.001

[21] Bignall, G., Milicich, S., Ramírez, L., Rosenberg, M., Kilgour, G. and Rae, A. (2010) Geology of the Wairakei-Tauhara Geothermal System, New Zealand. *Proceedings World Geothermal Congress* 2010, Bali, 25-29 April 2010, 30.

[22] Milicich, S.D., Rae, A.J., Rosenberg, M.D. and Bignall, G. (2008) Lithological and Structural Controls on Fluid Flow and Hydrothermal Alteration in the Western Ohaaki Geothermal Field (New Zealand)—Insights from Recent Deep Drilling. *Geothermal Resources Council, Transactions*, **32**, 303-307.

[23] Milicich, S.D., *et al*. (2010) Stratigraphic Correlation Study of the Kawerau Geothermal Field. GNS Science Consultancy, Confidential Report to Mighty River Power Limited 2010/23.

[24] Intergovernmental Panel on Climate Change (IPCC) (2023) Climate Change 2022—Impacts, Adaptation and Vulnerability. Cambridge University Press. https://doi.org/10.1017/9781009325844

[25] INSEED (2017) Annuaire des données du RGPH 2017: Populations cibles des programmes de développement.

[26] Flower, M.F.J. (1973) Trace-Element Distribution in Lavas from Anjouan and Grande

Comore, Western Indian Ocean. *Chemical Geology*, **12**, 81-98. https://doi.org/10.1016/0009-2541(73)90107-1

[27] Hajash, A. and Armstrong, R.L. (1972) Paleomagnetic and Radiometric Evidence for the Age of the Comores Islands, West Central Indian Ocean. *Earth and Planetary Science Letters*, **16**, 231-236. https://doi.org/10.1016/0012-821x(72)90195-1

[28] Emerick, C.M. and Duncan, R.A. (1982) Age Progressive Volcanism in the Comores Archipelago, Western Indian Ocean and Implications for Somali Plate Tectonics. *Earth and Planetary Science Letters*, **60**, 415-428. https://doi.org/10.1016/0012-821x(82)90077-2

[29] Nougier, J., Cantagrel, J.M. and Karche, J.P. (1986) The Comores Archipelago in the Western Indian Ocean: Volcanology, Geochronology and Geodynamic Setting. *Journal of African Earth Sciences* (1983), **5**, 135-145. https://doi.org/10.1016/0899-5362(86)90003-5

[30] Upton, B.G.J. (1982) Oceanic Islands. In: Nairn, A.E.M. and Stehli, F.G., Eds., *The Ocean Basins and Margins*, Springer US, 585-648. https://doi.org/10.1007/978-1-4615-8038-6_13

[31] Bachèlery, P. and Coudray, J. (1993) Carte géologique des Comores: Notice explicative de la carte volcano-tectonique de la Grande Comore (Ngazidja). Mission Française de la Copération.

[32] BRGM (1964) Rapport hydrogéologique sur l'alimentation en eau de la ville de Moroni (Grande Comore). BRGM, Tananarive, Technique 64 A/25.

[33] BRGM (1965) Alimentation en eau de la ville de Moroni (Grande Comore). Sondage de reconnaissance. BRGM, Tananarive, Technique 65 A/34.

[34] BRGM (1970) Alimentation en eau de Moroni (Grande Comore), Puits TP1. BRGM, Tananarive, Technique 70/22.

[35] BRGM (1972) Alimentation en eau de l'aérodrome de Hahaîa (Grande Comore) étude hydrogéologique et géophysique. BRGM, Tananarive, Technique 72/7.

[36] DCTD (1986) Recherche et mise en valeur des eaux souterraines, rapport technique, Hydrogéologie de l'île de Ngazidja (Grande Comore), état des connaissance en juillet 1986.

[37] DCTD (1987) Rapport technique des projets COI/79/005 et COI/86/001. Perspectives de mise en valeur des eaux souterraines pour l'alimentation en eau des agglomération de l'île de Ngazidja (Grande Comore). Moroni, Comore, Technique COI/79/005 et COI/86/001.

[38] DCTD (1988) Les eaux souterraines de l'Afrique orientale, centrale et australe. *Ressources Naturelles*, **19**, 50-67.

[39] Turner, R.J., Mansour, M.M., Dearden, R., Ó Dochartaigh, B.É. and Hughes, A.G. (2014) Improved Understanding of Groundwater Flow in Complex Superficial Deposits Using Three-Dimensional Geological-Framework and Groundwater Models: An Example from Glasgow, Scotland (UK). *Hydrogeology Journal*, **23**, 493-506. https://doi.org/10.1007/s10040-014-1207-0

[40] Artimo, A., Mäkinen, J., Berg, R.C., Abert, C.C. and Salonen, V. (2003) Three-dimensional Geologic Modeling and Visualization of the Virttaankangas Aquifer, Southwestern Finland. *Hydrogeology Journal*, **11**, 378-386. https://doi.org/10.1007/s10040-003-0256-6

[41] Cherry, D., Gill, B., Pack, T. and Rawling, T. (2011) Geoscience Australia and GeoScience Victoria: 3-D Geological Modeling Developments in Australia. 19-24. https://www.researchgate.net/publication/281786125_Geoscience_Australia_and_GeoScience_Victoria_3-D_Geological_Modeling_Develop-

ments_in_Australia

[42] Robins, N.S., Rutter, H.K., Dumpleton, S. and Peach, D.W. (2005) The Role of 3D Visualisation as an Analytical Tool Preparatory to Numerical Modelling. *Journal of Hydrology*, **301**, 287-295. https://doi.org/10.1016/j.jhydrol.2004.05.004

[43] Spottke, I., Zechner, E. and Huggenberger, P. (2005) The Southeastern Border of the Upper Rhine Graben: A 3D Geological Model and Its Importance for Tectonics and Groundwater Flow. *International Journal of Earth Sciences*, **94**, 580-593. https://doi.org/10.1007/s00531-005-0501-4

[44] Russell, H., *et al.* (2011) Three-Dimensional Geological Mapping for Groundwater Applications. In: Berg, R.C., Mathers, S.J., Kessler, H. and Keefer, D.A., Eds., *Synopsis of Current Three-Dimensional Geological Mapping and Modeling in Geological Survey Organizations*, Illinois State Geological Survey, 92.

[45] Thomsen, R. (2011) 3D Groundwater Mapping in Denmark Based on Calibreted High Resolution Airborne Geophysical Data. Workshop Extended Abstract, Geological Society of America. https://pub.geus.dk/en/publications/3d-groundwater-mapping-in-denmark-based-on-calibreted-high-resolu

[46] White (2013) Development of Three-Dimensional Models of Sedimentary Lithologies and Piezometric Levels to Understand Groundwater and Surface Water Flows, Lower Wairau Plain, Marlborough, New Zealand with Web and Smart Phone Access to Model Data. https://www.semanticscholar.org/paper/DEVELOPMENT-OF-THREE-DIMENSIONAL-MODELS-OF-AND-TO-%2C-White/b48be325761c5b0c9569a2e2593bfdc9efd36d9f

[47] Åberg, S.C., Åberg, A.K. and Korkka-Niemi, K. (2021) Three-Dimensional Hydrostratigraphy and Groundwater Flow Models in Complex Quaternary Deposits and Weathered/Fractured Bedrock: Evaluating Increasing Model Complexity. *Hydrogeology Journal*, **29**, 1043-1074. https://doi.org/10.1007/s10040-020-02299-4

[48] Voss, C.I. and Souza, W.R. (1987) Variable Density Flow and Solute Transport Simulation of Regional Aquifers Containing a Narrow Freshwater-Saltwater Transition Zone. *Water Resources Research*, **23**, 1851-1866. https://doi.org/10.1029/wr023i010p01851

[49] Buchanan, S. and Triantafilis, J. (2009) Mapping Water Table Depth Using Geophysical and Environmental Variables. *Groundwater*, **47**, 80-96. https://doi.org/10.1111/j.1745-6584.2008.00490.x

[50] Rabah, F.K.J., Ghabaye, S.M. and Salha, A.A. (2011) Effect of GIS Interpolation Techniques on the Accuracy of the Spatial Representation of Groundwater Monitoring Data in Gaza Strip. *Journal of Environmental Science and Technology*, **4**, 579-589. https://doi.org/10.3923/jest.2011.579.589

[51] Caruso, C. and Quarta, F. (1998) Interpolation Methods Comparison. *Computers & Mathematics with Applications*, **35**, 109-126. https://doi.org/10.1016/s0898-1221(98)00101-1

[52] Webster, R. (2001) Geostatistics for Environmental Scientists. John Wiley & Sons. http://archive.org/details/geostatisticsfor0000webs

[53] Bouhata, R., Kalla, M. and Driddi, H. (2015) Cartographie de la variabilité spatiale de la salinité du sol dans de la zone endoréique de Gadaine (Nord-Est algérien). *Romanian Journal of Geography*, **59**, 63-69.

[54] Collins, F.C. and Bolstad, P.V. (1996) A Comparison of Spatial Interpolation Techniques in Temperature Estimation. *Proceedings of the Third International Confer-*

ence/ Workshop on Integrating GIS and Environmental Modeling, Santa Fe, 21-25 January 1996.

[55] Johnston, K., Krivoruchko, K. and Lucas, N. (2004) Using ArcGIS Geostatistical Analyst. ESRI, 300.

[56] Nalder, I.A. and Wein, R.W. (1998) Spatial Interpolation of Climatic Normals: Test of a New Method in the Canadian Boreal Forest. *Agricultural and Forest Meteorology*, **92**, 211-225. https://doi.org/10.1016/s0168-1923(98)00102-6

[57] Akramkhanov, A., Martius, C., Park, S.J. and Hendrickx, J.M.H. (2011) Environmental Factors of Spatial Distribution of Soil Salinity on Flat Irrigated Terrain. *Geoderma*, **163**, 55-62. https://doi.org/10.1016/j.geoderma.2011.04.001

[58] Pyrcz, M. and Deutsch, C. (2003) The Whole Story on the Hole Effect. Geostatistical Association of Australasia.

[59] Delhomme, J.P. (1978) Kriging in the Hydrosciences. *Advances in Water Resources*, **1**, 251-266. https://doi.org/10.1016/0309-1708(78)90039-8

[60] ESRI (2025) Utilisation de la validation croisée pour évaluer les résultats d'interpolation. https://pro.arcgis.com/fr/pro-app/3.3/help/analysis/geostatistical-analyst/performing-cross-validation-and-validation.htm

[61] Triki Fourati, H., Bouaziz, M., Benzina, M. and Bouaziz, S. (2017) Detection of Terrain Indices Related to Soil Salinity and Mapping Salt-Affected Soils Using Remote Sensing and Geostatistical Techniques. *Environmental Monitoring and Assessment*, **189**, Article No. 177. https://doi.org/10.1007/s10661-017-5877-7

[62] Arslan, H. (2012) Spatial and Temporal Mapping of Groundwater Salinity Using Ordinary Kriging and Indicator Kriging: The Case of Bafra Plain, Turkey. *Agricultural Water Management*, **113**, 57-63. https://doi.org/10.1016/j.agwat.2012.06.015

[63] Tabasaki, K. and Mink, J. (1983) Volcano Feeder Dikes Impound Large Resources of Groundwater in the Hawaîan Island. *International Conference on Groundwater and Management*, Sydney, 5-9 December 1983, 309-318.

[64] Lau, L.S. and Mink, J.F. (2006) Hydrology of the Hawaiian Islands. University of Hawaii Press.

[65] SONEDE (2023) Rapport annuel d'exploitation des eaux souterraines de l'île de la Grande Comore. Société Nationnalle d'Exploitation et de Distribution des Eaux (SONEDE).